Molecular and environmental cues in cardiac differentiation of mesenchymal stem cells

Ramkisoensing, A.A.

CHAPTER III

FORCED ALIGNMENT OF MESENCHYMAL STEM CELLS UNDERGOING CARDIOMYOGENIC DIFFERENTIATION AFFECTS FUNCTIONAL INTEGRATION WITH CARDIOMYOCYTE CULTURES

Daniël A. Pijnappels[1], *Martin J. Schalij*[1], *Arti A. Ramkisoensing*[1], *John van Tuyn*[1,2], *Antoine A. F. de Vries*[2], *Arnoud van der Laarse*[1], *Dirk L. Ypey*[1], *Douwe E. Atsma*[1].

Departments of Cardiology[1], and Molecular Cell Biology[2], Leiden University Medical Center, Leiden, The Netherlands.

Circ Res. 2008 Jul 18;103(2):167-76.

ABSTRACT

Alignment of cardiomyocytes (CMCs) contributes to the anisotropic (direction-related) tissue structure of the heart, thereby facilitating efficient electrical and mechanical activation of the ventricles. This study aimed to investigate the effects of forced alignment of stem cells during cardiomyogenic differentiation on their functional integration with CMC cultures.

Labeled neonatal rat (nr) mesenchymal stem cells (MSCs) were allowed to differentiate into functional heart muscle cells in different cell-alignment patterns during 10 days of co-culture with nrCMCs. Development of functional cellular properties was assessed by measuring impulse transmission across these stem cells between two adjacent nrCMC fields, cultured onto micro-electrode arrays and previously separated by a laser-dissected channel (230±10 mm) for nrMSC transplantation. Coatings in these channels were micro-abraded in a direction (1) parallel, or (2) perpendicular to the channel, or (3) left unabraded, to establish different cell patterns.

Application of cells onto micro-abraded coatings resulted in anisotropic cell alignment within the channel. Application on unabraded coatings resulted in isotropic (random) alignment. Upon co-culture, conduction across seeded nrMSCs occurred from day 1 (perpendicular and isotropic) or day 6 (parallel) onward. Conduction velocity (CV) across nrMSCs at day 10 was highest in the perpendicular (11±0.9 cm/s,n=12), intermediate in the isotropic (7.1±1 cm/s,n=11), and lowest in the parallel configuration (4.9±1 cm/s,n=11) ($p<0.01$). nrCMCs and fibroblasts served as positive and negative control, respectively. Also, immunocytochemical analysis showed alignment-dependent increases in Cx43 expression.

In conclusion, forced alignment of nrMSCs undergoing cardiomyogenic differentiation affects the time course and degree of functional integration with surrounding cardiac tissue.

INTRODUCTION

The developing heart is characterized by increases in the number and size of cells resulting from hyperplasia and hypertrophy.[1,2] During this process, the initially round-shaped cardiomyocytes (CMCs) become elongated through unidirectional growth and align in a specific direction, thereby defining a long and short cellular axis.[3] Later in development, intercalated disc components (including gap junction proteins), initially distributed more or less uniformly over the surface of the cells, cluster at the polar ends of the cells.[4,5] Consequently, the elongated terrace-shaped cells are coupled end-to-end to surrounding cells and organized in unit bundles. This anisotropic tissue architecture has implications for the electrical activation of the cardiac muscle. Conduction of the electrical impulse parallel to the myocardial fiber axis is about 3 times faster than perpendicular to the fiber axis, indicating anisotropic conduction.[6] In the intact heart, the resulting inhomogeneity in conduction is circumvented by a ~120 degrees rotation of the fiber axis from epi- to endocardium. As a consequence the spread of activation through the ventricular muscle is more or less homogeneous, coordinated and fast.[7,8] Any disruption of this architecture, for example after myocardial infarction, may cause conduction abnormalities, associated with diminished pump function and increased risk of arrhythmias.[9]

Recently, stem cell therapy has been introduced as a treatment option to improve left ventricular function after myocardial infarction.[10] Ideally, to be successful, stem cells should not only differentiate into CMCs but also engraft and align with the surrounding anisotropic tissue. This latter process can be referred to as spatial integration. As a result, these *de novo* CMCs will be an integral part of the 3-dimentional myocardial architecture, thereby contributing to cardiac impulse conduction. Until now it is unknown how transplanted stem cells integrate with the surrounding myocardial cells, and to which extent alignment of these cells may influence electrical conduction. In other words, spatial integration of stem cell-derived CMCs may contribute to restoration of tissue structure and conduction or, in contrast, result in increased structural and electrical inhomogeneity. In theory, each cell type that is coupled electrically, excitable, and aligned can acquire anisotropic properties as in this situation the resistance in the transverse direction is higher than in the longitudinal direction. In case of stem cells this is of special interest as they may acquire anisotropic properties during cardiomyogenic differentiation after they have been transplanted into the anisotropic myocardium, thereby potentially improving their functional integration with the surrounding myocardium. Of note, functional integration of such transplanted cells is essential for cell therapy to be safe and effective.[11]

In the present study, we used a standardized 2-dimensional *in vitro* co-incubation model with a growth-directing substrate,[12,13] to investigate the effects of cell alignment on functional integration and electrical conduction across neonatal rat (nr) mesenchymal stem cells (MSCs) undergoing cardiomyogenic differentiation. The process of differentiation occurred in a cardiac syncytium of neonatal rat cardiomyocytes (nrCMCs) thereby allowing the study of functional integration.

MATERIALS AND METHODS

Animal experiments were approved by the Animal Experiments Committee of the Leiden University Medical Center and conformed to the Guide for the Care and Use of Laboratory Animals as stated by the US National Institutes of Health.

A detailed description of harvesting and culturing of nrCMCs, nrMSCs, and cardiac fibroblasts (nrCFBs), as well as the characterization of the nrMSCs can be found in the online Data Supplement.

ASSESSMENT OF FUNCTIONAL CARDIOMYOGENESIS

Differentiation of nrMSCs was assessed by a combination of immunofluorescence microscopy and electrophysiological measurements in isotropic co-cultures of nrCMCs and eGFP-labeled nrMSCs grown on glass coverslips during the course of 10 days. The assessment of cardiomyogenesis by immunofluorescence and intracellular measurements is described in the online Data Supplement.

MICRO-ELECTRODE HIGH-DENSITY MAPPING

Simultaneous micro-electrode high density mapping of cultured nrCMCs and nrMSCs was performed using micro-electrode arrays (MEA, number of titanium nitride electrodes: 60; inter-electrode distance: 200 mm; electrode diameter: 30 mm) and associated data acquisition system (sampling rate 5 kHz/channel, Multi Channel Systems, Reutlingen, Germany). Further descriptions can be found in the online Data Supplement.

INDUCTION OF CONDUCTION BLOCK AND ANISOTROPIC CELL ALIGNMENT

Activation maps of nrCMCs were generated 2 days after culture to confirm the presence of a synchronously beating monolayer. Conduction block was generated using a P.A.L.M. microlaser system (Microlaser Technologies GmbH, Bernried, Germany).[14] Briefly, two pre-programmed linear laser dissections were made, separated by 225 μm, crossing the entire diameter of the monolayer in the coated MEA culture dish. This resulted in a detached strip of monolayer between the two laser dissection lines, which was removed from the culture, creating a clean a-cellular

channel electrically separating the two nrCMC fields. Subsequently, the uncovered coatings in the a-cellular channels were given a micro-groove pattern by micro-abrasion[15] with a soft micro-brush (bristle diameter: 30 mm diameter) using a micro-manipulator (Seizz, Göttingen, Germany) and light-microscope (40x magnification), either in a direction (1) parallel or (2) perpendicular to the a-cellular channel. Another group (3) consisted of MEA culture dishes with an a-cellular channel that was not micro-abraded.

After confirming the presence of a conduction block between the two nrCMC fields, either (a) $5x10^4$ CM-DiI-labeled nrCMCs, (b) $5x10^4$ eGFP-labeled nrMSCs or (c) $5x10^4$ eGFP-labeled nrCFBs were applied in a channel-crossing pattern in each of the three groups. This was achieved by gently adding the cells onto the coating in-between the CMC fields, using a pipette fixed to a micro-manipulator in combination with a light-microscope (20x magnification). After 24 h, the culture medium was refreshed to remove non-attached cells, as well as 1 h before and after measurements. During the following 10 days the electrical conduction (impulse transmission) across seeded cells was assessed daily.

The two separated and asynchronously beating nrCMC fields were considered electrically coupled upon application of cells, if the timing of the electrograms of the two nrCMC fields correlated consistently with each other for 30 consecutive LATs recorded at both fields, while stimulating one nrCMC field.

In an additional series of experiments, a mixture of $5x10^4$ nrCMCs and nrCFBs (20%:80%) was applied to the channel and subjected to electrophysiological measurements 24 h after seeding and served as positive control for the results obtained in the nrMSC group at day 10.

STATISTICS

Statistical analysis was performed using SPSS 11.0 for Windows (SPSS Inc., Chicago, IL, USA). Data were compared with Student's t-test or ANOVA test with Bonferroni correction for multiple comparisons, and expressed as mean±SD for a given number (n) of observations. P-values <0.05 were considered statistically significant.

RESULTS

CHARACTERIZATION OF BONE MARROW-DERIVED NEONATAL RAT MESENCHYMAL STEM CELLS

Analysis of in vitro adipogenic and osteogenic differentiation potential

The nrMSCs (Fig 1, A1) were assessed for their multipotency by investigating their adipogenic and osteogenic differentiation potential. After incubation in appropriate differentiation media, nrMSCs readily differentiated into adipocytes and osteoblasts, as determined by formation of lipid vacuoles and calcium deposits, respectively (Fig 1, A2-3).

Analysis of surface marker and connexin expression

A very large fraction of the nrMSCs (p2) expressed the mesenchymal markers CD29 (97.3%), and CD90 (96.2%) at their surface, while almost none of them stained positive for the hematopoietic marker CD34 (1.5%). CD44 (32.8%), CD45 (10.2%), and CD106 (10.3%) were expressed in a small to medium sized fraction of nrMSCs (Fig 1, B).[16]

After 3 days of culture, nrMSCs showed positive staining for Cx43 ($220\pm26x10^3$ intensity units (iu) in 1024 pixel x 768 pixel image) and Cx45 ($149\pm9x10^3$ iu) inside the cell and at cell-cell contacts, whereas Cx40 staining was hardly detectable ($15\pm7x10^3$ iu) (Fig 2, A1-3). At day 10, positive staining for Cx43, Cx40, and Cx45 had increased significantly ($p<0.01$, Fig 2, E), without a noticeable change in their distribution patterns (Fig 2, C1-3).

In co-cultures of nrCMCs and eGFP-labeled nrMSCs, the latter cells stained positive for Cx43 ($291\pm15x10^3$ iu) and Cx45 ($204\pm9x10^3$ iu) in a dense punctuated pattern at day 3 of culture, with Cx40 being hardly detectable ($19\pm9x10^3$ iu) (Fig 2, B1-3). At day 10 after cell seeding, only Cx43 and Cx45 staining had significantly increased ($p<0.01$) as compared to day 3 of culture, but distribution patterns did not changed over time. In contrast, no increase in Cx40 staining was observed in or between cells at day 10 of culture (Fig 2, D1-3).

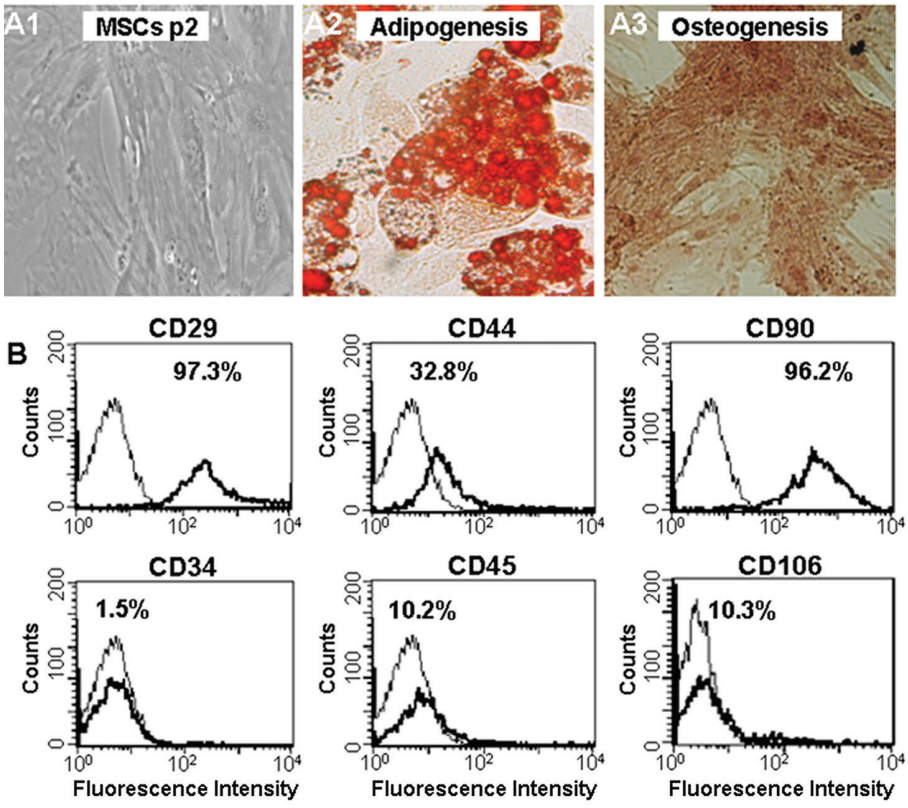

Figure 1. Characterization of neonatal rat mesenchymal stem cells (nrMSCs). A1, Brightfield image of cultured nrMSCs. A2, presence of Oil Red O-stained fat vacuoles after adipogenic differentiation. A3, calcium accumulation was visualized by Alizarine Red S staining after osteogenic differentiation. B, Flow cytometric analysis of nrMSCs showed abundant surface expression of CD29 and CD90, but hardly any expression of the hematopoietic marker CD34. Furthermore, CD44, CD45 and CD106 were expressed at low or medium levels. Flow cytometric analyses with isotype-matched control antibodies are included to determine background fluorescence levels (thin black line).

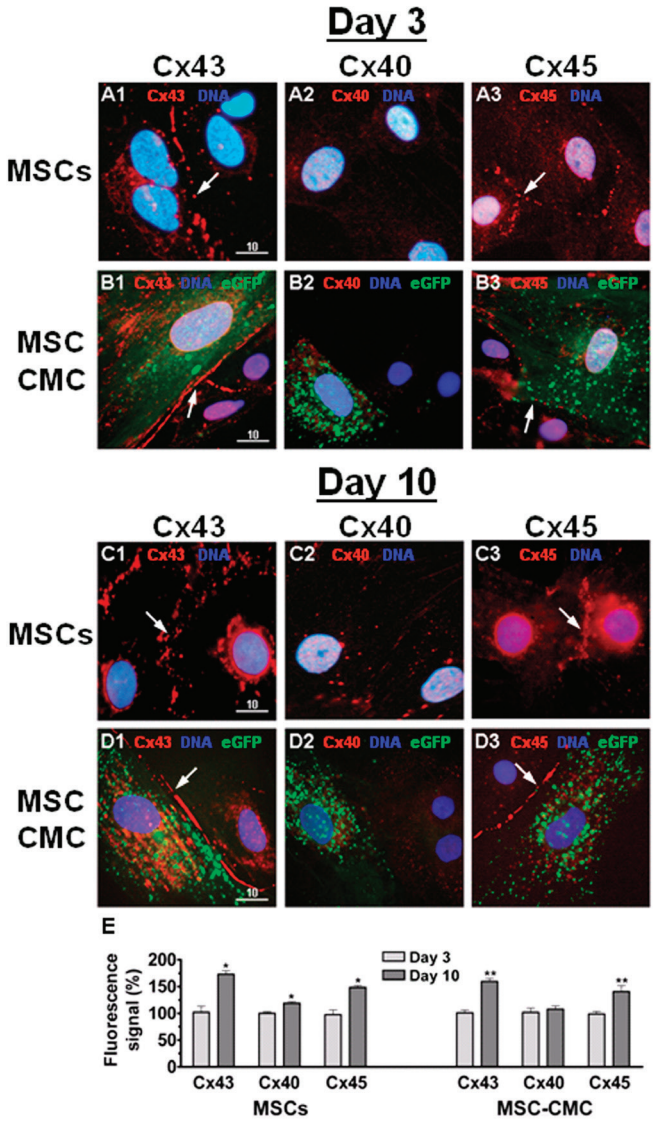

Figure 2. Immunocytochemical analysis of connexin (Cx) staining in isotropic co-cultures of neonatal rat mesenchymal stem cells (nrMSCs) and nrCMCs at day 3 and day 10 of culture. Staining for Cx43 and Cx45 increased significantly over time in nrMSCs (A1, A3, C1 and C3) as well as in nrMSCs adjacent to nrCMCs (B1, B3, D1 and D3). Positive staining for Cx40 increased only in MSCs during follow-up (A2 and C2). Quantitative analysis (E) was based on 36 random samples taken from 12 adjacent nrMSC-nrMSC and nrCMC-nrMSC cell pairs on 3 different coverslips at each time point. White arrows pinpoint the presence of Cxs at the site of gap junctions. *p<0.01 vs. nrMSCs at day 3, **p<0.01 vs. nrMSC-nrCMC pairs at day 3.

ASSESSMENT OF CARDIOMYOGENIC DIFFERENTIATION

Immunocytochemistry

At day 3 of co-culture, a fraction of the eGFP-labeled nrMSCs stained positive for sarcomeric α-actinin and cardiac troponin-I in a diffuse and speckled staining pattern (Fig 3, A2 and A4).

However, a larger fraction of nrMSCs stained negative for both markers (Fig 3, A1 and A3). Cross-striation in nrMSCs was first observed at day 6, while at day 10, ~17% of the eGFP-labeled nrMSCs showed typical cardiac cross-striated patterns of sarcomeric α-actinin (Fig 3, D1-3) and cardiac troponin-I (Fig 3, D4-6). Most of the nrMSCs displaying cross-striation were adjacent to native CMCs. Importantly, none of the nrMSCs having cross-striation of contractile proteins (>60 cells analyzed per sarcomeric protein type) were heterokaryomeric, making cell fusion of eGFP-labeled cells with nrCMCs unlikely. Total positive staining for sarcomeric α-actinin and cardiac troponin-I in eGFP-labeled cells increased significantly from 34±5% and 30±6% at day 3, to 63±3% and 60±4% at day 10 (now including 17.1±3% and 16.3±4% of cells that show positive staining with cross-striation), respectively ($p<0.001$) (Fig 3, B). Furthermore, sarcomere length (i.e. distance between two Z-lines) in differentiated nrMSCs at day 10 was comparable to that in native nrCMCs (Fig 3, C1-2). Samples having irregularities in sarcomere structures (less than 10% of samples) were excluded.

Electrophysiological measurements after uncoupling

Patch-clamp recordings were obtained from nrCMCs and eGFP-labeled nrMSCs at day 3 and day 10 of co-culture after electrical isolation with the gap junction uncoupler 2-aminoethoxydiphenyl borate (2-APB). Upon 2-APB treatment, the synchronously beating monolayer disintegrated into asynchronously beating cells, and input resistance increased from 20-120 MW (n=15) to 0.9-1.2 GW (18 other cells). These increases in input resistances were considered to reflect electrical uncoupling of the patched cell from the surrounding cells, thereby reaching the approximate seal resistance.[17] After electrical uncoupling at day 3, eGFP-labeled nrMSCs (n=9) had maximal diastolic potentials of -16±5 mV and showed no spontaneous action potentials (APs). In contrast, uncoupled nrCMCs (n=12) had maximal diastolic potentials of -69±8 mV in the presence of spontaneous APs.

Interestingly, after 10 days of co-culture and incubation with 2-APB, a considerable fraction of nrMSC-derived nrCMCs (~16%, n=9) was found to be beating independently from surrounding nrCMCs (as judged by timing and frequency of beating), while showing AP characteristics (maximal diastolic potential: -63±4 mV) comparable to native nrCMCs (n=10) (Fig 4, A1-2, B1-4). The remaining nrMSCs (n=47) were non-beating and had a maximal diastolic potential of -19±4 mV, in the absence of APs (Fig 4, A2).

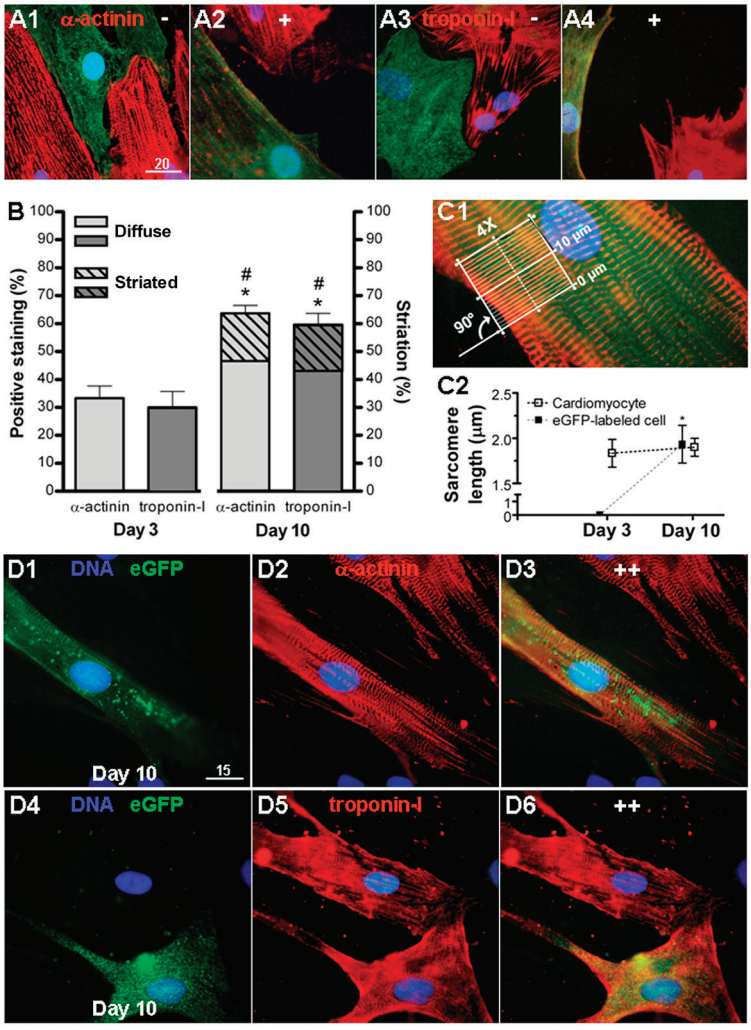

Figure 3. Cardiomyogenic differentiation of neonatal rat mesenchymal stem cells (nrMSCs) co-cultured with nrCMCs assessed by immunocytochemistry. A fraction of eGFP-labeled nrMSCs stained negative for (A1) sarcomeric α-actinin and (A3) cardiac troponin-I at day 3 of culture. However, other nrMSCs stained positive for (A2) sarcomeric α-actinin and (A4) cardiac troponin-I, which percentage increased significantly over time (B). At day 10 of co-culture, positive staining in typical cardiac cross-striated pattern was observed for both (D1-6) sarcomeric α-actinin and cardiac troponin-I in 17.1±3% and 16.3±4% of the nrMSCs, respectively (B). (C1-2) Estimation of sarcomere lengths in native nrCMCs and eGFP-labeled cells showed no significant difference. Quantitative analysis was based on 360 cells per sarcomeric protein at each time point. *P<0.01, vs. percentage positive staining at day 3. #P<0.01, vs. percentage cross-striation at day 3.

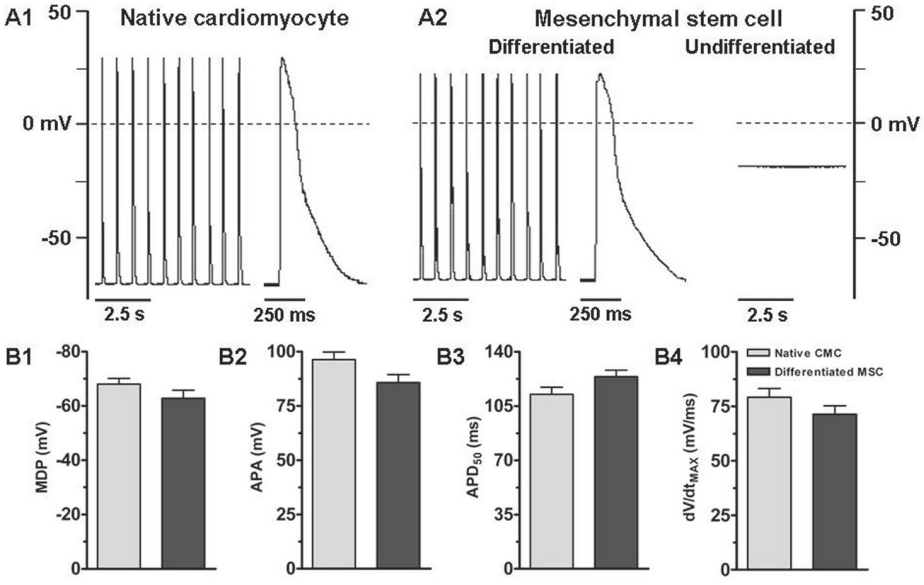

Figure 4. Whole-cell patch-clamp recordings from nrCMCs and eGFP-labeled neonatal rat mesenchymal stem cells (nrMSCs) after 10 days of co-culture and gap junction uncoupling. Stable and spontaneous action potentials were recorded in (A1) nrCMCs (n=10), as well as in (A2, left panel) differentiated eGFP-labeled cells (n=9). In contrast, undifferentiated, non-beating nrMSCs had resting membrane potentials of -19±4 mV, in the absence of action potentials (A2, right panel; n=47). Action potential characteristics were comparable to each other, as shown by maximum diastolic potential (MDP, B1); action potential amplitude (APA, B2); action potential duration till 50% repolarization (APD_{50}, B3) and maximal rate of depolarization (dV/dt_{MAX}, B4).

CELL ALIGNMENT AFTER MICRO-ABRASION

Only confluent monolayers with a high degree of structural and functional homogeneity were included in this study as determined by light-microscopy and electrophysiological mapping. Furthermore, damaged and/or detached nrCMC fields, due to laser dissection or micro-abrasion, were excluded from the study. As a consequence only 40% of the cultures were included for further experiments.

Application of nrCMCs, nrMSCs or nrCFBs onto the uncovered fibronectin-gelatin coating in the a-cellular channel resulted in a confluent, isotropic cell layer (Fig 5, A1). Micro-abrasion of the coating, either parallel or perpendicular to the channel, resulted in alignment of each cell type according to the direction of abrasion (Fig 5, B1 and C1). nrMSCs, as other applied cells, appeared elongated with an average length-width ratio of 4:1 and maintained their shape throughout follow-up

(Fig 5, D1-2). In contrast, cells applied onto unabraded coatings had a variable length-width ratio (Fig 5, D3), but never reaching 4:1 of anisotropically aligned cells.

EFFECT OF CELL ALIGNMENT ON CONDUCTION VELOCITY AND FUNCTIONAL INTEGRATION

After creating an a-cellular channel (230±10 μm) in the MEA culture dish, two asynchronously beating nrCMC fields were present, proving the presence of a conduction block. CV across the two isotropic nrCMC fields was 21.3±2.3 cm/s at day 1, and increased slightly to 22.7±2.6 cm/s at day 10.

Isotropic cell alignment

Application of nrCMCs onto unabraded coatings in the channels resulted in conduction between the two nrCMC fields within 1 day. CV across nrCMCs in the channel was 19.7±0.7 cm/s at day 1 and 20.7±1 cm/s at day 10 (n=12, NS) (Fig 5, A2), which was comparable to the CV values measured across neighboring nrCMC fields (Fig 6, A1).

Application of nrMSCs in the channel also restored conduction between both nrCMC fields, but CV was significantly lower: 1.7±0.7 cm/s ($p<0.01$). CV across these isotropically aligned nrMSCs increased to 7.1±1 cm/s at day 10 (n=11, $p<0.01$) (Fig 5, A2 and Fig 6, A1). Electrical conduction between the nrCMC fields was also restored after application of nrCFBs, however, CV across these cells was 1.8±0.8 cm/s at day 1 and remained stable till day 10 (n=12, NS and Fig 6, A1), being significantly lower than the CV across nrMSCs at day 10 ($p<0.01$) (Fig 5, A2).

Anisotropic cell alignment: parallel versus perpendicular cell alignment

Application of nrCMCs onto coatings abraded in a direction parallel to the channel resulted, after 1 day, in electrical recoupling of the two nrCMC fields, which was associated with a CV of 13.5±0.9 cm/s across the nrCMC-filled channel and persisted during follow-up (CV: 14.1±1 cm/s, n=10, NS) (Fig 5, B2 and Fig 6, B1). Application of nrCMCs onto coatings abraded in a direction perpendicular to the channel, however, resulted in a CV of 26.0±1.1 cm/s ($p<0.01$) across the channel, which also persisted during the follow-up till day 10 (CV: 26.8±0.9 cm/s, n=11, NS) (Fig 5, C2 and Fig 6, C1).

In contrast, application of nrMSCs onto coatings abraded in a direction parallel to the channel failed to restore electrical conduction between the two nrCMC fields up to day 7. However, at day 7, restoration had occurred and was associated with a CV of 4.9±1 cm/s at day 10 (n=11, $p<0.01$) (Fig 5, B2 and Fig 6, B1). Application of nrMSCs onto perpendicularly abraded coatings restored electrical conduction between the two nrCMC fields from day 1 onward. CV increased from 4.3±1 cm/s at day 1 to 11±0.9 cm/s at day 10 (n=12, $p<0.01$) (Fig 5, C2 and Fig 6, C1), thereby

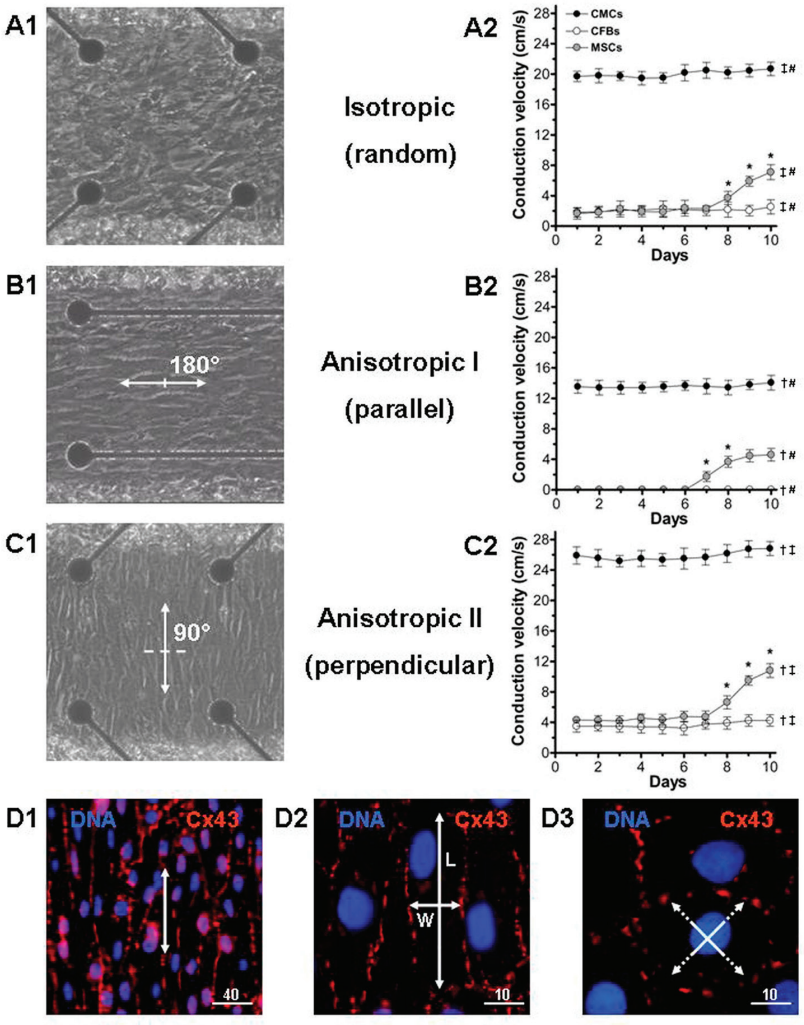

Figure 5. The effect of cell alignment on the development of conduction across the cell strip displaying a random, parallel or perpendicular configuration. (D1) Cells applied on micro-abraded coatings showed typical alignment throughout follow-up. (D2) After alignment, neonatal rat mesenchymal stem cells (nrMSCs) appeared elongated with oval shaped nuclei (average length-width ratio of 4:1, L=length, W=width), and displayed Cx43 staining uniformly distributed along cell-cell contacts. (D3) In contrast, application of cells onto unabraded coatings resulted in random cell alignment, with a variable length-width ratio (but always lower than the 4:1), which was maintained till day 10. Two-factor mixed ANOVA test (Bonferroni-corrected); †$p<0.01$ vs. CV at day 10 in random configuration, ‡$p<0.01$ vs. CV at day 10 in parallel configuration, #$p<0.01$ vs. CV at day 10 in perpendicular configuration. One-way repeated-measures ANOVA (Bonferroni-corrected); *$p<0.05$.

reaching the highest CV in the nrMSC group in the different configurations (isotropic: 7.1±1 cm/s and parallel: 4.9±1 cm/s at day 10). This indicates that alignment of nrMSCs undergoing cardiomyogenic differentiation influences the degree of functional integration with respect to CV across adjacent cardiac tissue.

Application of nrCFBs onto the parallel abraded coatings did not result in electrical conduction between the two nrCMC fields during 10 days of culture (n=10, $p<0.0001$) (Fig 5, B2 and Fig 6, B1). However, after application of nrCFBs in perpendicular abraded coatings, electrical conduction was restored at day 1, associated with a CV across these cells of 3.5±0.8 cm/s at day 1 and 4.3±1 cm/s at day 10 (n=10, NS) (Fig 5, C2 and Fig 6, C1).

Interestingly, quantitative analysis of Cx43 in different cells, configurations, and locations at day 10 of culture showed significant differences, revealing that the highest Cx43 expression was found in the group of parallel alignment (Fig 6, corresponding panels A2, B2, and C2).

The degree of cell alignment and confluence did not change significantly over time, as was shown by quantification and spatial measurements using (immuno) fluorescence microscopy (data not shown).

Conduction velocity across control cultures of cardiomyocyte/fibroblast mixtures

In order to mimic the composition of the cell population in the channel at day 10, which consisted of nrMSCs-derived CMCs and undifferentiated nrMSCs (~18% and ~82%, respectively), mixtures of native nrCMCs and nrCFBs (20% and 80%) were applied in all three different configurations (n=8, 8 and 9). After application of these mixtures onto the coatings, CVs determined at day 1 were comparable to CVs across eGFP-labeled nrMSCs at day 10 of culture (n=11, 10 and 10) (Fig 7). This suggests that the increase in CV across eGFP-labeled MSCs that was observed depends on the functional cardiomyogenic differentiation of nrMSCs.

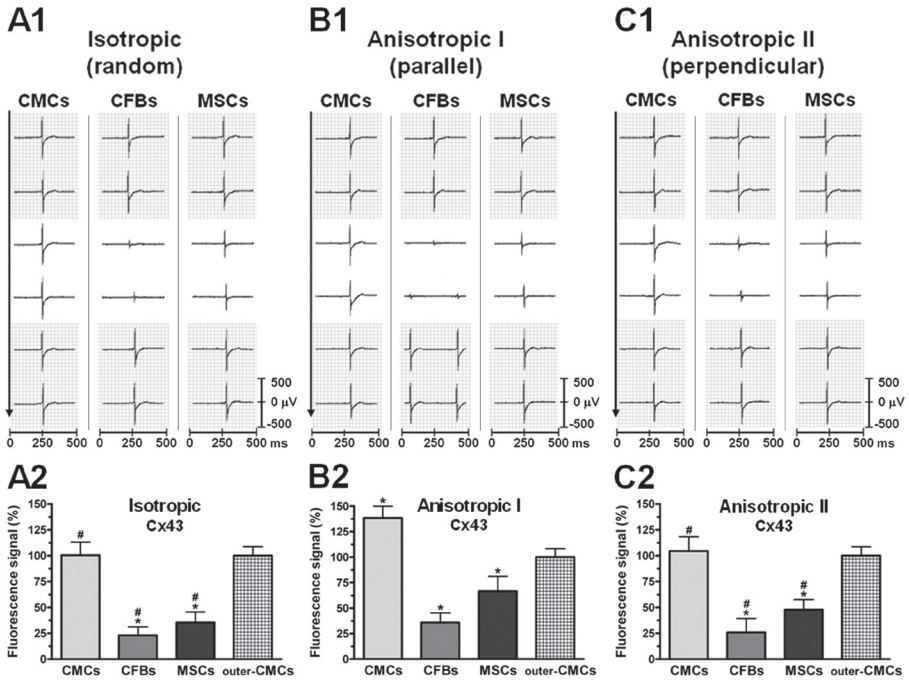

Figure 6. (A1-C1) Extracellular electrograms derived from 10-day old cultures of neonatal rat cardiomyocytes (nrCMCs), cardiac fibroblasts (nrCFBs), or mesenchymal stem cells (nrMSCs) cultured in different configurations and from different locations (white background). In grey, electrograms of adjacent cardiomyocyte fields are shown, and referred to as outer-CMCs. (A2-C2) Cx43 expression was quantified in all three cell types and compared to expression in adjacent cardiomyocyte fields (gritted bars for outer-CMCs, set to 100%). Cx43 expression was also quantified and compared between all three cell types in each configuration. *$p<0.05$ vs Cx43 expression of outer-CMCs, #$p<0.05$ vs Cx43 expression in corresponding cells aligned parallel to the channel.

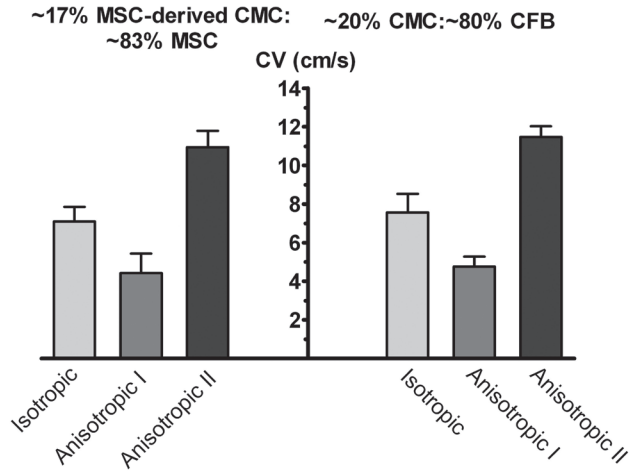

Figure 7. Positive control for cardiomyogenesis-related increase in CV across neonatal rat mesenchymal stem cells (nrMSCs). CVs across nrMSCs at day 10, cultured in one of the three configurations (n=11, 10 and 10), were compared to CVs across a mixture of 20% nrCMCs and 80% neonatal rat cardiac fibroblasts at day 1 (n=8, 8 and 9).

DISCUSSION

The present study shows that alignment of transplanted neonatal rat mesenchymal stem cells (nrMSCs) undergoing cardiomyogenic differentiation affects the time course and degree of functional integration with cultured neonatal rat cardiomyocyte tissue.

Functional differentiation of neonatal rat mesenchymal stem cells

In this study, a significant fraction of nrMSCs differentiated into functional cardiomyocytes upon co-culture with nrCMCs. In additional co-culture experiments, differentiation percentages of nrMSCs were assessed at day 14, showing ~18% differentiation (compared to ~17% differentiation at day 10), which may indicate that maximal differentiation percentages were reached under our culture conditions. Previously, Nishiyama *et al.* also showed the cardiomyogenic differentiation potential of premature MSCs upon co-culture with CMCs.[18] The results of our study confirm these results using nrMSCs and nrCMCs. In addition, Jiang *et al.* demonstrated that MSCs from young rats differentiated into cardiac-like cells after transplantation in the infarcted rat myocardium, whereas MSCs from old rats did not.[19]

In the present study, differentiation of nrMSCs into functional cardiomyocytes was also demonstrated by intracellular (patch-clamp) membrane potential recordings after uncoupling. One might argue that the 2-APB-induced uncoupling in the patch-clamp experiments may be incomplete and that 180 mmol/L 2-APB may have affected plasma membrane ion channels, thereby affecting excitability of the nrCMCs and differentiated nrMSCs. However, the observed desynchronized beating and high whole-cell input resistance (~1 GW) in the presence of 2-APB indicated preserved single-cell excitability and strong uncoupling. These findings, together with the presence of cardiomyocyte-like action potentials in the uncoupled differentiated nrMSCs but not in uncoupled undifferentiated nrMSCs are indicative for functional differentiation of at least a fraction of the nrMSCs.

Alignment of stem cell-derived cardiomyocytes and electrical conduction

Several studies have shown anisotropic conduction across aligned CMCs *in vitro*. The longitudinal and transverse CVs measured across nrCMCs in this study are in line with the results of previous studies using the same source,[13] although some studies have reported higher CVs.[15,20] These differences in CV might have been caused by the presence of different numbers of cardiac fibroblasts in the CMC culture, or by the methods used to produce anisotropic cell cultures.[13] However, in our study, we also applied other cells than CMCs to the micro-abraded coatings and these also appeared elongated with oval shaped nuclei and a certain level of Cx43 uniformly distributed along cell-cell contacts. Anisotropic alignment of cells in our model most likely created a low-resistance conduction pathway in longitudinal direction, where fewer (high resistance) cell borders have to be crossed, thereby favoring conduction in this direction. These phenomena were not restricted to a specific cell type. However, after culture and cardiomyogenic differentiation of nrMSCs the anisotropic electrical properties further developed and functional integration with adjacent cardiomyocyte fields improved. The anisotropic ratio (perpendicular CV vs parallel CV) was comparable between nrCMCs and nrMSCs at day 10 of culture, however only CV across nrMSCs increased over time.

Distribution patterns of Cx43 did not appear to be of major influence on conduction, which has been confirmed by other studies.[15,21] The uniform distribution of Cx43 in nrCMCs, reported in the present and other studies, is typical for neonatal CMCs. Importantly, cells aligned parallel to the channel, thereby having adjacent, beating cardiac tissue perpendicular to their cell axis, were associated with the highest increase in Cx43 expression levels. A previous study reporting on neonatal CMCs subjected to anisotropic stretch showed a higher increase in Cx43 expression in CMCs stretched perpendicular to their cell axis than when CMCs

were stretched in a parallel direction.[22] In our model, the cells in the channel seem to be influenced by stretch originating from the adjacent cardiomyocyte fields, thereby indicating that alignment per se is not only affecting functional integration but that it also has an effect on gap junction regulation. In fact, our model could allow the study of stretch-related protein expression levels, as alternative to mechanically induced pulsatile stretch, which also was shown to significantly increase Cx43 expression in nrCMCs.[23] In addition, cardiomyogenic differentiation of nrMSCs may lead to increased Cx expression. Also, long-term culturing of MSCs itself leads to upregulation of Cx expression.[24] However, the relative contributions of each of these phenomena to the improvement of AP transmission by increased gap junctional coupling warrants further study.

In the present study, nrMSCs in all three cell orientation groups showed a time-dependent increase in CV which correlated with differentiation of nrMSCs, although the maximum CV differed among the groups. Comparison of the CV values of the transplanted nrMSCs with CV values of nrCMCs at different time points revealed the effect of stem cell alignment on functional integration with cardiac tissue. This is best illustrated by the finding that non-excitable nrMSCs aligned parallel to the channel were unable to conduct the electrical current across the channel for up to 6 days. However, after cardiomyogenic differentiation of these cells, electrical conduction across the channel was established. Most likely, in this situation passive conduction across non-differentiated nrMSCs is supported by active propagation across nrMSC-derived CMCs, resulting in AP transmission across the channel and subsequent activation of the distal CMC field. Thus, the alignment of stem cells not only influences the degree of functional integration, as reflected by CV values, but also the time course of functional integration. Whether alignment also influenced the degree of cardiomyogenic differentiation in itself is intriguing. The minor differences between CVs across mixtures of native nrCMCs and nrCFBs and CVs across differentiated nrMSCs indicate that alignment per se is a major determinant of functional integration. However, the increased expression of Cx43 in the nrMSCs aligned to the channel could suggest that alignment has some effect on cardiomyogenic differentiation, but this increase may also be due to the factors mentioned above. Future studies will be necessary to investigate the role of cell alignment in cardiomyogenic differentiation and subsequent effects on structural and electrical integration.

Possible therapeutic implications

To our knowledge, no study of stem cell transplantation has yet reported on the effects of cell alignment on electrical conduction, functional integration and the therapeutic implications. Furuta *et al.* have used transplanted sheets of nrCMCs onto the epicardial surface of the heart to improve cardiac function and showed

anisotropic electrical conduction across the cell sheets.[25] Interestingly, these cells appeared to orientate themselves spontaneously in line with the fiber axis of native cells. However, it is unknown whether and how stem cells align after transplantation into the myocardium of the infarcted heart, and to which extent alignment of these cells is influencing conduction and contraction. Of note, alignment of resident ventricular CMCs has major influence on electrical and mechanical activation of the heart,[26] but the cellular assessment *in vivo* is technically challenging. The present study introduces alignment of transplanted stem cells as a novel determinant of functional integration, and although conducted *ex vivo*, the study may have important implications for future cardiac cell therapy. Presumably, cell alignment will become even more important in the near future, as higher engraftment rates of transplanted cells will be achieved using novel application techniques. For example, misalignment of transplanted cells with respect to the native cardiac architecture might result in increased electrical heterogeneity potentially leading to arrhythmias as well as dyssynchronous contraction leading to decreases in cardiac output.[9] On the other hand, enforcing transplanted cells to adapt to the native tissue architecture might contribute to improved therapeutic efficiency and safety. In this view, an important and promising role is reserved for tissue engineering, in which the transplanted cells can be aligned with the use of scaffolds.[27,28]

Study limitations

Ideally, the nrCMC fields adjacent to the channel should be made anisotropic to mimic cardiac tissue architecture. This was however not possible with the techniques described in the study. Although the spatial resolution of the extracellular mapping experiments is acceptable to allow standardized measurements, the relatively low spatial resolution may have resulted in an underestimation of actual CVs. In the present study, a growth-directing substrate was created by micro-abrasion and although effective and reproducible, this procedure is time-consuming and yields only a limited number of cultures suitable for further study. Nevertheless, our study provides the first evidence that alignment of stem cells undergoing cardiomyogenic differentiation has significant impact on functional integration of these cells with cardiac tissue.

CONCLUSIONS

Forced alignment of nrMSCs undergoing cardiomyogenic differentiation affects the time course and degree of functional integration with surrounding host cardiac tissue. This study introduces cell alignment as an important determinant of functional integration of transplanted cells, which may contribute to the improvement

of therapeutic outcome and reduction of potential hazards. Further study is needed to determine the full biological, biophysical, and therapeutic relevance of cell alignment in functional integration of transplanted cells with host myocardium.

REFERENCES

1. Li F, Wang X, Capasso JM, Gerdes AM. Rapid transition of cardiac myocytes from hyperplasia to hypertrophy during postnatal development. *J Mol Cell Cardiol.* 1996;28:1737-1746.
2. Oparil S, Bishop SP, Clubb FJ, Jr. Myocardial cell hypertrophy or hyperplasia. *Hypertension.* 1984;6:III38-III43.
3. Hirschy A, Schatzmann F, Ehler E, Perriard JC. Establishment of cardiac cytoarchitecture in the developing mouse heart. *Dev Biol.* 2006;289:430-441.
4. Angst BD, Khan LU, Severs NJ, Whitely K, Rothery S, Thompson RP, Magee AI, Gourdie RG. Dissociated spatial patterning of gap junctions and cell adhesion junctions during postnatal differentiation of ventricular myocardium. *Circ Res.* 1997;80:88-94.
5. Gourdie RG, Green CR, Severs NJ, Thompson RP. Immunolabelling patterns of gap junction connexins in the developing and mature rat heart. *Anat Embryol (Berl).* 1992;185:363-378.
6. Saffitz JE, Kanter HL, Green KG, Tolley TK, Beyer EC. Tissue-specific determinants of anisotropic conduction velocity in canine atrial and ventricular myocardium. *Circ Res.* 1994;74:1065-1070.
7. Streeter DD, Jr., Spotnitz HM, Patel DP, Ross J, Jr., Sonnenblick EH. Fiber orientation in the canine left ventricle during diastole and systole. *Circ Res.* 1969;24:339-347.
8. Wiegner AW, Bing OH, Borg TK, Caulfield JB. Mechanical and structural correlates of canine pericardium. *Circ Res.* 1981;49:807-814.
9. Peters NS, Wit AL. Myocardial architecture and ventricular arrhythmogenesis. *Circulation.* 1998;97:1746-1754.
10. Orlic D, Hill JM, Arai AE. Stem cells for myocardial regeneration. *Circ Res.* 2002;91:1092-1102.
11. Leobon B, Garcin I, Menasche P, Vilquin JT, Audinat E, Charpak S. Myoblasts transplanted into rat infarcted myocardium are functionally isolated from their host. *Proc Natl Acad Sci U S A.* 2003;100:7808-7811.
12. Fast VG, Kleber AG. Microscopic conduction in cultured strands of neonatal rat heart cells measured with voltage-sensitive dyes. *Circ Res.* 1993;73:914-925.
13. Bursac N, Parker KK, Iravanian S, Tung L. Cardiomyocyte cultures with controlled macroscopic anisotropy: a model for functional electrophysiological studies of cardiac muscle. *Circ Res.* 2002;91:e45-e54.
14. Pijnappels DA, van Tuyn J, de Vries AA, Grauss RW, van der Laarse A, Ypey DL, Atsma DE, Schalij MJ. Resynchronization of separated rat cardiomyocyte fields with genetically modified human ventricular scar fibroblasts. *Circulation.* 2007;116:2018-2028.
15. Fast VG, Kleber AG. Anisotropic conduction in monolayers of neonatal rat heart cells cultured on collagen substrate. *Circ Res.* 1994;75:591-595.
16. Pittenger MF, Martin BJ. Mesenchymal stem cells and their potential as cardiac therapeutics. *Circ Res.* 2004;95:9-20.
17. Harks EG, Camina JP, Peters PH, Ypey DL, Scheenen WJ, van Zoelen EJ, Theuvenet AP. Besides affecting intracellular calcium signaling, 2-APB reversibly blocks gap junctional coupling in confluent monolayers, thereby allowing measurement of single-cell membrane currents in undissociated cells. *FASEB J.* 2003;17:941-943.

18. Nishiyama N, Miyoshi S, Hida N, Uyama T, Okamoto K, Ikegami Y, Miyado K, Segawa K, Terai M, Sakamoto M, Ogawa S, Umezawa A. The significant cardiomyogenic potential of human umbilical cord blood-derived mesenchymal stem cells in vitro. *Stem Cells.* 2007;25:2017-2024.
19. Jiang S, Kh HH, Ahmed RP, Idris NM, Salim A, Ashraf M. Transcriptional profiling of young and old mesenchymal stem cells in response to oxygen deprivation and reparability of the infarcted myocardium. *J Mol Cell Cardiol.* 2008;44:582-596.
20. Fast VG, Darrow BJ, Saffitz JE, Kleber AG. Anisotropic activation spread in heart cell monolayers assessed by high-resolution optical mapping. Role of tissue discontinuities. *Circ Res.* 1996;79:115-127.
21. Spach MS, Heidlage JF, Barr RC, Dolber PC. Cell size and communication: role in structural and electrical development and remodeling of the heart. *Heart Rhythm.* 2004;1:500-515.
22. Gopalan SM, Flaim C, Bhatia SN, Hoshijima M, Knoell R, Chien KR, Omens JH, McCulloch AD. Anisotropic stretch-induced hypertrophy in neonatal ventricular myocytes micropatterned on deformable elastomers. *Biotechnol Bioeng.* 2003;81:578-587.
23. Zhuang J, Yamada KA, Saffitz JE, Kleber AG. Pulsatile stretch remodels cell-to-cell communication in cultured myocytes. *Circ Res.* 2000;87:316-322.
24. Pijnappels DA, Schalij MJ, van Tuyn J, Ypey DL, de Vries AA, van der Wall EE, van der Laarse A, Atsma DE. Progressive increase in conduction velocity across human mesenchymal stem cells is mediated by enhanced electrical coupling. *Cardiovasc Res.* 2006;72:282-291.
25. Furuta A, Miyoshi S, Itabashi Y, Shimizu T, Kira S, Hayakawa K, Nishiyama N, Tanimoto K, Hagiwara Y, Satoh T, Fukuda K, Okano T, Ogawa S. Pulsatile cardiac tissue grafts using a novel three-dimensional cell sheet manipulation technique functionally integrates with the host heart, in vivo. *Circ Res.* 2006;98:705-712.
26. Hooks DA, Tomlinson KA, Marsden SG, LeGrice IJ, Smaill BH, Pullan AJ, Hunter PJ. Cardiac microstructure: implications for electrical propagation and defibrillation in the heart. *Circ Res.* 2002;91:331-338.
27. Radisic M, Park H, Shing H, Consi T, Schoen FJ, Langer R, Freed LE, Vunjak-Novakovic G. Functional assembly of engineered myocardium by electrical stimulation of cardiac myocytes cultured on scaffolds. *Proc Natl Acad Sci U S A.* 2004;101:18129-18134.
28. Feinberg AW, Feigel A, Shevkoplyas SS, Sheehy S, Whitesides GM, Parker KK. Muscular thin films for building actuators and powering devices. *Science.* 2007;317:1366-1370.

EXPANDED MATERIALS AND METHODS

ISOLATION AND CULTURE OF NEONATAL RAT CARDIOMYOCYTES AND CARDIAC FIBROBLASTS.

All animal experiments were approved by the Animal Experiments Committee of the Leiden University Medical Center and conformed to the Guide for the Care and Use of Laboratory Animals as stated by the US National Institutes of Health.

Cardiomyocytes (CMCs) were dissociated from ventricles of 2-day old male neonatal (nr) Wistar rats and grown in culture medium supplemented with 5% horse serum (HS, Invitrogen, Carlsbad, CA, USA), penicillin (100 U/mL) and streptomycin (100 µg/mL; P/S; Bio-Whittaker, Verviers, Belgium), as previously described [1].

Before their use in cell pattern experiments, nrCMCs were collected in culture flasks and labeled with the viable fluorescent dye chloromethylbenzamido (CM-DiI) (CellTrackerä, Molecular Probes, Eugene, OR, USA) according to the recommendations of the manufacturer.

Micro-electrode array culture dishes (MEA, Multi Channel Systems, Reutlingen, Germany) and glass coverslips were pre-coated for 4 h with fibronectin-gelatin (8:2, $^{v}/_{v}$, 0.1% fibronectin and gelatin in PBS), and dried using pressurized nitrogen. nrCMCs were plated ($1.5x10^{6}$ cells) on MEAs or on glass coverslips in 6-well culture dishes ($2x10^{6}$ cells/well) and incubated in a humidified incubator at 37° C and 5% CO_2 to obtain confluent spontaneously beating monolayer of nrCMCs.

In addition, adherent neonatal rat cardiac fibroblasts (nrCFBs) were collected, purified (by re-plating), enhanced green fluorescent protein (eGFP)-labeled and cultured in a 1:1 ($^{v}/_{v}$) mixture of Dulbecco's modified Eagle's medium (DMEM, Invitrogen) and Ham's F10 medium (ICN Biomedicals, Irvine, CA, USA) supplemented with 10% fetal bovine serum (FBS, Invitrogen), penicillin (100 U/mL) and streptomycin (100 µg/mL). CFBs were labeled with eGFP using the vesicular stomatitis virus G protein-pseudotyped self-inactivating lentivirus vector CMVPRES [2] essentially as described by van Tuyn *et al* [3].

Proliferation of residual nrCFBs in nrCMC cultures was inhibited by incubation with 100 mmol/L 5-bromo-2-deoxyuridine (BrdU, Sigma-Aldrich, Saint Louis, MO, USA) in culture medium during the first 24 after culture initiation.

HARVESTING AND CHARACTERIZATION OF BONE MARROW-DERIVED NEONATAL RAT MESENCHYMAL STEM CELLS AND CARDIOMYOGENIC DIFFERENTIATION.

Harvesting

Bone marrow was isolated from *femora* and *tibiae* of the same 2-day-old male Wistar rats used for nrCMC harvesting. Marrow was extruded from the bones by centrifugation at 13,000 rpm for 30 s (rotor diameter: 15 cm), suspended in 10 mL

of stem cell medium [human mesenchymal stem cell growth medium (MSCGM) consisting of 440 ml basal medium, 50 ml of mesenchymal growth supplements, 15% FBS (Invitrogen), 4 mmol/L of L-glutamine, penicillin (50 U/L) and streptomycin (50 mg/L), amphothericin B solution (1 mL/mL, Sigma-Aldrich) (Cambrex Bio Science, Walkersville, MD, USA)], and 6% heparin (400 IE/ml). This suspension was centrifuged again at 1000 rpm for 10 min. Next, the pellet was resuspended in 7 ml of this medium supplemented with 5.75 µg/mL deoxyribonuclease I (DNase, Sigma-Aldrich). The cells were then plated in 25-cm^2 culture flasks (Becton Dickinson, Franklin Lakes, NJ, USA) and incubated at 37° C and 5% CO_2 for 2 days after which non-adherent cells were removed. Stem cell medium was refreshed twice a week until the primary cultures of nrMSCs were confluent, after which they were expanded by serial passage. In this study passages 2 to 4 were used. To ensure identification, nrMSCs were transduced with CMVPRES as described earlier in this section.

CHARACTERIZATION OF NRMSCS

Adipogenic and osteogenic differentiation of mesenchymal stem cells

The nrMSCs were characterized by established differentiation assays[4]. Briefly, $5x10^3$ nrMSCs per well were plated in a 12-well culture plate, and exposed to adipogenic or osteogenic induction medium. Adipogenic differentiation medium consisted of a regular culture medium (DMEM supplemented with 15% FBS, 100 U/L penicillin and 100 µg/mL streptomycin, 1 µg/mL amphothericin B solution) supplemented with 5 µg/mL insulin, 1 µmol/L dexamethason, 50 µmol/L indomethacin and 0.5 µmol/L 3-isobutyl-1-methylxanthine (IBMX) (all from Sigma-Aldrich), and was refreshed every 3-4 days for a period of 3 weeks. Lipid accumulation was assessed by Oil Red O staining of the cultures (15 mg Oil Red O/mL 60% isopropanol) and light microscopy. Osteogenic differentiation medium consisted of culture medium supplemented with 10 mmol/L b-glycerophosphate, 50 µg/mL ascorbic acid and 10 nmol/L dexamethason (all from Sigma-Aldrich), and was refreshed every 3-4 days for a period of 2 weeks. Afterwards, the cells were washed with phosphate-buffered saline (PBS), and calcium deposits were visualized by staining of the cells for 2-5 min with 2% Alizarine Red S in 0.5% NH_4OH (pH 5.5).

Flow cytometry

Analysis of surface marker expression was carried out by flow cytometry. The nrMSCs were detached using trypsin/EDTA (Bio-Whittaker) and resuspended in PBS containing 0.5% bovine serum albumine (BSA, Sigma-Aldrich), and divided in aliquots of $5x10^4$ cells. Cells were then incubated for 30 min at 4°C with fluorescein isothiocyanate (FITC)- or phycoerythrin (PE)-conjugated antibodies against

rat CD34 (Santa Cruz Biotechnology, Santa Cruz, CA, USA), CD29, CD44, CD45, CD90, CD106 (Becton Dickinson). Labeled cells were washed and analyzed using a FACSort flow cytometer (Becton Dickinson), equipped with a 488-nm argon ion laser and a 635-nm red diode laser. Isotype-matched control antibodies (Becton Dickinson) were used to determine background fluorescence. At least $5x10^3$ cells per sample were acquired and data were processed using CellQuest software (Becton Dickinson).

IMMUNOCYTOLOGICAL ANALYSIS OF GAP JUNCTION CONTENT AND CARDIOMYOGENIC DIFFERENTIATION POTENTIAL

Isotropic co-cultures of $2x10^6$ nrCMCs and $5x10^4$ eGFP-labeled nrMSCs were stained for cardiac connexins and sarcomeric proteins on day 3 or day 10 after culture initiation. To detect sarcomeric proteins, we used mouse monoclonal antibodies specific for sarcomeric α-actinin (Sigma-Aldrich) or mouse anti-cardiac troponin I (HyTest Ltd., Turku, Finland), both at a dilution of 1:400. Rabbit polyclonal anti-connexin 40 (Cx40), anti-Cx43 and anti-Cx45 antibodies were used to stain gap junctional proteins, and examined as previously described.[1] In addition, anisotropic co-cultures were stained for Cx43 to show the effects of anisotropic cell alignment on Cx distribution in nrMSCs. In these cultures, cellular distribution and quantity of Cx43 were studied by the use of fixed Areas of Interest (AOI) which were placed on both longitudinal and transversal sides of the cells (n=32 for each cell type in each configuration). In each AOI the fluorescent spots were quantified using dedicated software (Image-Pro Plus, Version 4.1.0.0, Media Cybernetics, Silver Spring, MD, USA), this allowed us the estimate global distribution of Cx staining. An AOI covering the whole cell-area was used in cultures of isotropic cell alignment. The primary antibodies were visualized with rabbit anti-mouse IgG or goat anti-rabbit IgG Alexa antibodies (Invitrogen). Unless stated otherwise, antibodies were used at a dilution of 1:200.

The percentage of eGFP-labeled cells showing positive staining for sarcomeric proteins was calculated by quantification of 6 cultures (60 cells per culture per sarcomeric protein, at 40x magnification) at each time point, using a threshold value of 50 on the 0-255 intensity scale. To assess structural integrity, sarcomere lengths in native nrCMCs and eGFP-labeled cells were estimated from 64 standardized individual measurements (4 areas of 20μmx20μm per cell). The area of measurement covered the cell-surface aspect of in total 8 native nrCMCs and 8 eGFP-labeled cells that exhibited typical sarcomeric α-actinin cross-striation without any observable inhomogeneities. A fluorescence microscope equipped with a digital camera (Nikon Eclipse, Nikon Europe, Badhoevedorp, The Netherlands) and dedicated software (Image-Pro Plus, Version 4.1.0.0, Media Cybernetics, Silver Spring, MD, USA) were used to analyze data. All co-cultures of nrCMCs and eGFP-labeled

nrMSCs were stained using the same solutions, and equal exposure times. Quantifications were performed by an independent investigator.

ELECTROPHYSIOLOGICAL MEASUREMENTS IN PHARMACOLOGICALLY UNCOUPLED CELL MONOLAYERS

Whole-cell patch-clamp measurements were performed in co-cultures of $5x10^4$ eGFP-labeled nrMSCs and $2x10^6$ nrCMCs. To perform single-cell measurements from eGFP-labeled nrMSCs in a syncytium of beating nrCMCs, cells were pharmacologically uncoupled by incubation with 180 µmol/L of 2-aminoethoxydiphenyl borate (2-APB) (Tocris, Ballwin, MO, USA) for 15 min. This agent largely,[5] or fully[6] blocks gap junctional intercellular coupling by Cx40, Cx43, and Cx45. Whole-cell current-clamp recordings were performed at 25°C using a L/M-PC patch-clamp amplifier (3 kHz filtering) (List-Medical, Darmstadt, Germany) 3 and 10 days after culture initiation. Pipette solution contained (in mmol/L) 10 Na_2ATP, 115 KCl, 1 $MgCl_2$, 5 EGTA, 10 HEPES/KOH (pH 7.4). Tip resistance was 2.0 - 2.5 MW, and seal resistance >1 GW. The bath solution contained (in mmol/L) 137 NaCl, 4 KCl, 1.8 $CaCl_2$, 1 $MgCl_2$, 10 HEPES (pH 7.4). For data acquisition and analysis pClamp/Clampex8 software (Axon Instruments, Molecular Devices, Sunnyvale, CA, USA) was used. Action potentials were analyzed and compared between nrCMCs and eGFP-labeled nrMSCs. We did not correct for an existing tip potential during the membrane potential measurements, because this tip potential is assumed to be relatively small (~3 mV) for our bath and pipette solutions.[7] Input resistance of whole-cells coupled to their surrounding cells was measured in voltage-clamp by dividing the applied voltage steps by the stationary membrane current change.[6]

Micro-electrode high-density mapping

Electrograms were analyzed off-line using MC-Rack software (version 3.5.6, Multi Channel Systems). Electrical stimulation of cell cultures was performed via an external pipette electrode producing bipolar rectangular pulses (1.5x threshold, pulse width 10 ms), placed ~1 mm above the cell culture and >5 mm away from the measurement sites. Cultures were stimulated for at least 30 s, before recordings were started.

The maximal negative intrinsic deflection was taken as local activation time (LAT) and used to construct 2-dimensional color-coded activation maps (S-plus, version 6.2, Insightful Corporation, Seattle, WA, USA). Conduction velocities were calculated from averaged LATs recorded at 8 fixed measuring points, distributed equally over the two lines of electrodes adjacent to the channel.[1,8]

REFERENCES

1. Pijnappels DA, Schalij MJ, van Tuyn J, Ypey DL, de Vries AA, van der Wall EE, van der Laarse A, Atsma DE. Progressive increase in conduction velocity across human mesenchymal stem cells is mediated by enhanced electrical coupling. *Cardiovasc Res.* 2006;72:282-291.
2. Seppen J, Rijnberg M, Cooreman MP, Oude Elferink RP. Lentiviral vectors for efficient transduction of isolated primary quiescent hepatocytes. *J Hepatol.* 2002;36:459-465.
3. van Tuyn J, Pijnappels DA, de Vries AA, de V, I, van der Velde-van Dijke, Knaan-Shanzer S, van der Laarse A, Schalij MJ, Atsma DE. Fibroblasts from human postmyocardial infarction scars acquire properties of cardiomyocytes after transduction with a recombinant myocardin gene. *FASEB J.* 2007;21:3369-3379.
4. Pittenger MF, Mackay AM, Beck SC, Jaiswal RK, Douglas R, Mosca JD, Moorman MA, Simonetti DW, Craig S, Marshak DR. Multilineage potential of adult human mesenchymal stem cells. *Science.* 1999;284:143-147.
5. Bai D, del Corsso C, Srinivas M, Spray DC. Block of specific gap junction channel subtypes by 2-aminoethoxydiphenyl borate (2-APB). *J Pharmacol Exp Ther.* 2006;319:1452-1458.
6. Harks EG, Camina JP, Peters PH, Ypey DL, Scheenen WJ, van Zoelen EJ, Theuvenet AP. Besides affecting intracellular calcium signaling, 2-APB reversibly blocks gap junctional coupling in confluent monolayers, thereby allowing measurement of single-cell membrane currents in undissociated cells. *FASEB J.* 2003;17:941-943.
7. E. Neher. Correction for Liquid Junction Potentials in Patch Clamp Experiments. In: Rudy B and Iverson LE, eds. *Methods in Enzymology, volume 207, Ion Channels,* eds. New York, London: Academic Press; 1992.
8. Pijnappels DA, van Tuyn J, de Vries AA, Grauss RW, van der Laarse A, Ypey DL, Atsma DE, Schalij MJ. Resynchronization of separated rat cardiomyocyte fields with genetically modified human ventricular scar fibroblasts. *Circulation.* 2007;116:2018-2028.